

Comparison of a dynamic model and experimental results of a residential heat pump with vapor injection and variable speed scroll compressor

Bertrand Dechesne^a, Samuel Gendebien^a, Vincent Lemort^a, Stéphane Bertagnolio^b

^a *Thermodynamics Laboratory, Liège, Belgium, bdechesne@ulg.ac.be*

^b *Emerson Climate Technologies, Aachen, Germany, Stephane.Bertagnolio@Emerson.com*

Abstract:

The first part of this paper presents a Modelica-based dynamic model of the system. Finite-volume models are used for the heat exchangers and the evaporator model takes into account frost formation. A thermodynamic model of the vapor injection scroll compressor is developed using empirical correlations for the volumetric efficiency, isentropic efficiency and the ratio between the injection and suction mass flow rate.

The second part presents experimental results of a vapor injection and variable speed scroll compressor air to water residential heat pump. The unit is a 10kW residential system working with R410a as working fluid and capable of providing floor heating and domestic hot water. It was tested in a controlled environment in order to achieve a wide range of outdoor, including frosting conditions, and indoor conditions. The model predictions and experimental results are compared in order to validate the component models in steady state.

The experimental investigations showed that there is room for improvement on the control side of the system and the developed model can be used in order to develop model based control of the injection and outdoor electronic expansion valves.

Keywords:

Air-to-water heat pump, experimental, vapor injection, variable speed, scroll compressor, modeling, Modelica.

1. Introduction

Tackling the global warming issue is one of the greatest challenge of our time. A possible way to decrease greenhouse gases emissions from the residential sector is the use of high efficiency electrical system for floor heating and domestic hot water. This is probably why the market share of heat pump systems has grown significantly in Europe in the past decades and, in residential applications, air-source heat pumps (ASHP) are usually considered due to their relatively low cost. Improving performances of ASHP has been and one option is the use of variable speed compressor and vapor injection. Xu et al. [14] gave a deep literature review on the later option.

Dynamic modeling of refrigeration systems has recently become possible to study thanks to the ever-increasing power of computational packages and processors. Dynamic modeling helps to develop and test new control strategies in order to increase the system performances. In this field, Rasmussen et al. provides a deep literature review and a complete simulation tutorial for the dynamic modeling of vapor compression cycles ([1] and [2]). Hongtao et al. ([3] and [4]) studied a flash tank injection heat pump and developed a model in Modelica language. However, the studied compressor is a fixed speed scroll compressor. In [4], the authors presented the validation of their dynamic models for both system start-up and shut-down procedures. Jiazhen et al. [5] evaluated the steady-state and transient behavior of a heat pump working with different low-GWP refrigerants (R32 and D2Y60). In 2011, Li et al. [6]

developed a dynamic model of a R134a automotive air-conditioning and showed the refrigerant mass migration during start-up and shut-down operations.

This paper presents experimental results and a Modelica-based dynamic model of an air source heat pump (ASHP) using a variable speed vapor injection scroll compressor and R410A as working fluid. This model is based on the open-source and open-access ThermoCycle library [7] for the model components and CoolProp for the fluid thermodynamic properties [8]. An empirical model of the vapor injection scroll compressor is developed using empirical correlations for the volumetric efficiency, isentropic efficiency and the ratio between the injection and suction mass flow rates. PID controllers are used to control the needle position of the electronic expansion valve in order to obtain a target superheat on the injection line and at the exhaust of the evaporator.

The studied system is a residential air-to-water heat pump. The compressor is variable speed and uses vapor injection in order to achieve higher pressure ratios and condensing pressures. The system is an internal heat exchanger (i.e. economizer) injection cycle type and is composed of two separated units (indoor and outdoor). The outdoor unit is composed of the evaporator and the main electronic expansion valve. Between these two units, split lines are present, one of these is the vapor line, between the evaporator and the compressor suction. The other one is the liquid split line and is located between the exhaust of the drive cooler and the inlet of the outdoor electronic expansion valve. These split lines can reach up to 20 meters and have a major impact on the system dynamics. The drive cooler is a small heat exchanger made up of an aluminium plate in contact with both refrigerant tubes and the drive electronic circuit in order to cool down the latter (see Fig. 2).

2. Modeling

This Section presents the model of the heat pump developed in the Modelica language. Fig. 1 shows the system model where the main components are taken into account. Some modelling assumptions have been made in order to simplify the system: the drive cooler, 4-way valve and pressure drops have been neglected.

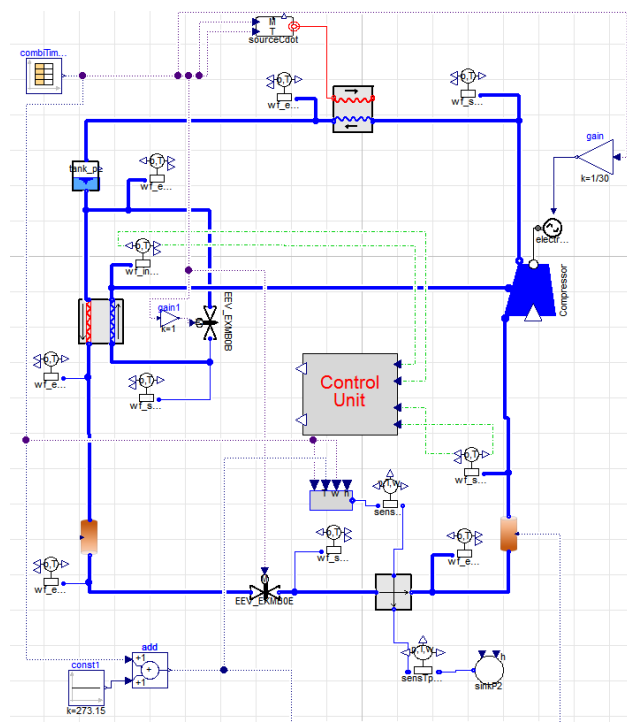


Fig. 1. Modelica model of the heat pump

2.1. Heat exchangers

Heat exchanger models are based on the finite volume method where the energy and mass conservation equations are applied to several cells connected in series, more information can be found in [7]. The dynamics taken into account in this model comes from the metal wall and the volume of fluid enclosed in the heat exchanger.

The fluid cells are thus connected to a metal wall with which heat is exchanged. However, no longitudinal conduction is taken into account. The main parameters of the dynamic heat exchangers models are the number of cells on each side, geometrical features such as the heat transfer area and the heat transfer coefficients (HTC) between both fluids and the metal wall. Different options are implemented to take into account the variation of the HTC (see [7]), in this case, a constant HTC in each zone (subcooled – two phase - superheated) was chosen. In fact, it was shown in [10] that, due to the low pinch point values, the heat transfer coefficient variations do not affect greatly the predicted heat transfer rate. This heat exchanger model is used for the condenser and economizer.

The split lines (refrigerant lines between the indoor and outdoor unit) model is based on the same fluid cells, which are also connected in series and to a metal wall representing the split line tube. These split lines are however buried in the ground in residential applications and are thus assumed to be adiabatic.

The evaporator model takes into account the moist air condensation using the Lewis analogy. Similarly to the condenser and economizer models, the refrigerant flow is divided into n fluid cells connected in series. In order to model the cross-flow heat exchanger, the air flow rate is divided into n cells in parallel. In this configuration, each air cell exchanges heat with one of the refrigerant cell. The temperature difference between the inlet and outlet of a refrigerant cell is quite small as the cells on the refrigerant side are in series, however, this remark is not correct on the air side as the cells are in parallel. The sensible heat exchange rate is thus computed using the $\varepsilon - NTU$ method and the latent heat exchange rate is determined via the Lewis analogy. The structure of the model is similar to the one for the condenser or economizer, a refrigerant cell is connected to a metal wall which is connected to an air cell.

A frost model is implemented in the moist air cell. This model is based on the work of Hermes et al. [14] and Lee et al. [9]. Most of the models in the literature are based on a series of assumptions:

- All processes (mass and heat transfer) are treated as a quasi-steady state and one dimensional phenomenon;
- The frost density is a layer-averaged value at any moment;
- The air pressure is uniform in the air stream and within the frost layer;
- The thermal conductivity of frost is a function of density;
- The frost thickness was assumed uniform along the wall;
- The Lewis analogy (analogy between heat and mass transfer) is applicable.

The model divides the overall mass flux into two parts, called the growth \dot{m}_g (contributing to increase the frost layer thickness) and the densification \dot{m}_d (contributing to increase the frost layer density) mass fluxes.

2.2. Compressor

The proposed model uses a set of five dimensionless polynomials to predict the compressor behavior. The compressor model is treated as quasi steady-state, in fact, the time constants associated to the compressor dynamics are very small compared to those associated with heat exchangers and charge distribution [5]. The inputs of the compressor polynomials are the rotational speed rpm and the three pressure levels, i.e. the suction pressure P_{su} , injection pressure P_{inj} and discharge pressure P_{ex} or combinations of these pressures, i.e.

$$r_{p,tot} = \frac{P_{ex}}{P_{su}} \quad , \text{ the total pressure ratio} \quad (1)$$

$$r_{p,inj} = \frac{P_{inj}}{P_{su}} \quad , \text{ the injection pressure ratio} \quad (2)$$

The mass flow rates, exhaust state and compressor consumption can be computed thanks to the five polynomials which are the volumetric and isentropic efficiencies (η_v and η_s), the drive efficiency (η_{drive}), the injection ratio (X_{inj}) and the losses ratio (X_{loss}). Finally, the model can be written as follows:

$$\dot{M}_{r,su} = \varepsilon_v(rpm, P_{su}, P_{inj}, P_{ex}) \cdot \rho_{r,su} \cdot V_s \cdot N_{rot} \quad (3)$$

$$\dot{M}_{r,inj} = X_{inj}(rpm, P_{su}, P_{inj}, P_{ex}) \cdot \dot{M}_{r,su} \quad (4)$$

$$\dot{W}_{in} = \frac{\dot{W}_s}{\varepsilon_s(rpm, P_{su}, P_{inj}, P_{ex})} \quad (5)$$

$$\dot{W}_s = \dot{M}_{r,su} \cdot (h_{r,ex,s} - h_{r,su}) + \dot{M}_{r,inj} \cdot (h_{r,ex,inj,s} - h_{r,inj}) \quad (6)$$

$$\dot{W}_{el} = \frac{\dot{W}_{in}}{\eta_{drive}(rpm, P_{su}, P_{inj}, P_{ex})} \quad (7)$$

$$\dot{Q}_{loss} = \dot{W}_{el} \cdot X_{loss}(rpm, P_{su}, P_{inj}, P_{ex}) \quad (8)$$

Where \dot{W}_{in} is the electrical power delivered to the compressor motor and \dot{W}_s the isentropic power. This latter is composed of two terms related to the isentropic compression of two separate volumes performing the compression process from the suction to the discharge pressure for the first one and from the injection to the discharge pressure for the second one. This model has been calibrated with manufacturer data and proved to predict the performance, mass flow rates and exhaust state accurately for two different scroll compressors as presented in more details in [10].

2.3. Expansion valves

Several electronic expansion valve (EEV) models are available in the literature. Most of the time, a correction coefficient is applied to the incompressible flow through a nozzle mass flow equation. This correction coefficient is a function of the working conditions of the valve. Bach et al. [11] developed a dimensionless law for the valve mass flow using the Buckingham PI-theorem. This law is valid for two-phase inlet conditions and for two refrigerants (R410a and R404a). Park et al. [12] also presented empirical laws for an EEV working with either R22 or R410a. The correlation yielded satisfactory predictions within a relative deviation of 15.0%. In the frame of this work, a new correlation for the

coefficient of correction C_d was developed thanks to the experimental campaign results. The mass flow rate passing through the valve is calculated as follows:

$$\dot{m}_{EEV} = C_d \cdot A_e \cdot \sqrt{2 \cdot \rho_{su,EEV} \cdot \Delta P_{EEV}} \quad (9)$$

Where

- A_e is the equivalent orifice area and is given by the full orifice area times the valve opening X_{open} . The valve full orifice area was measured, for both the main and injection expansion valve, on a laser cut expansion valve;
- $\rho_{su,EEV}$ is the density at the valve suction;
- ΔP_{EEV} is the pressure difference between the inlet and outlet of the valve.

As stated here above, the electronic expansion valves (EEV) have been studied by numerous authors. However, the correlations developed by Bach [11] and Park [12] were not adapted for the system studied in this paper. New correlations were developed for the discharge coefficient C_d of both the injection and outdoor EEVs thanks to experimental data. The goal is to develop a simple model of the valve in order to implement it in the whole system model. The mass flow is calculated via Eq.9 with a coefficient of determination given by the following equation:

$$C_d = a_0 \cdot \pi_1^{a_1} \quad (10)$$

Where π_1 is a dimensionless group equal to the ratio of the effective area over the full opening area of the valve, i.e. the valve opening. The parameters are given in Tab.1.

Table 1. Expansion valves parameters

Parameters	IEEV	OEEV
A_{full} [m ²]	1.227E-6	4.524E-6
a_0 [m ⁻¹]	0.918	0.2882
a_1 [-]	0.224	-0.638

2.4. Liquid receiver

This tank is placed at the exhaust of the condenser and is filled with saturated liquid and vapor. The liquid receiver is considered as one control volume and modeled using the energy and mass conservation principles assuming thermodynamic equilibrium at all times inside the control volume. No ambient losses are modeled. The refrigerant charge in the system is imposed by the initial conditions in the heat exchangers, split lines and tank. Hence, by varying the initial level in the liquid receiver, it is possible to adjust the total refrigerant charge in the cycle without changing the working conditions.

3. Experimental Set-up

The present section aims at describing the apparatus developed to carry out experimental investigations on the air-to-water heat pump. A schematic representation of the test bench is given in Fig. 2. The blue and red refrigerant lines are respectively only used in cooling or heating mode. However, in the rest of the paper, the reversible heat pump is supposed to work only in heating mode.

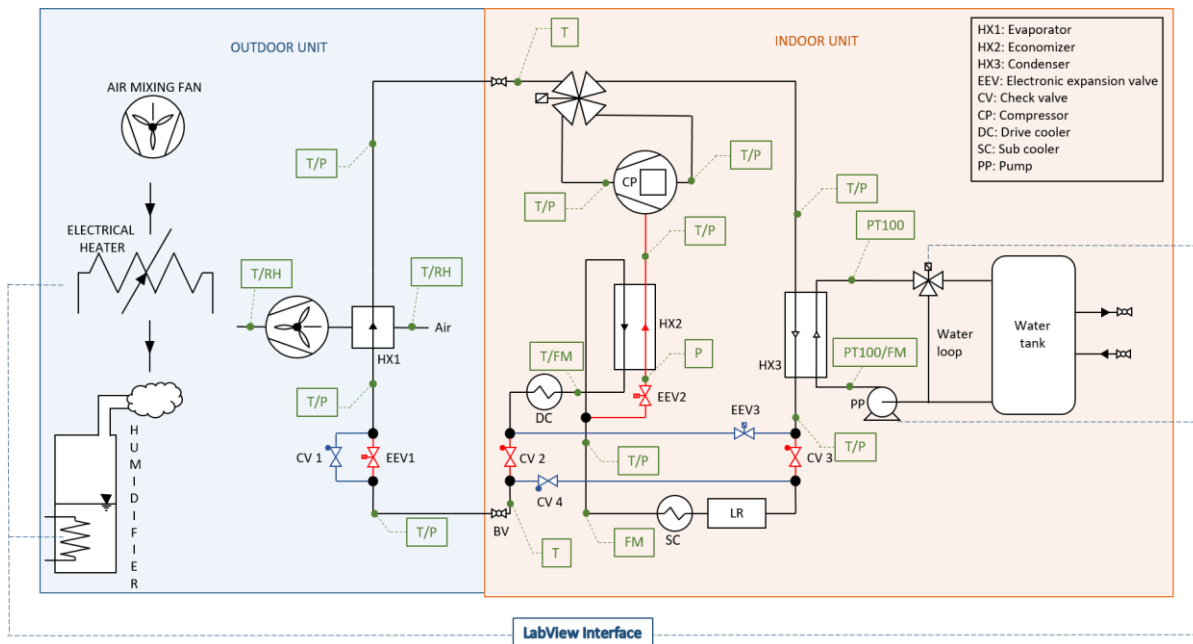


Fig. 2. Schematic representation of the test bench

3.1. Refrigerant loop

The refrigerant loop is controlled by means of a ModBus Interface, which implies the adjustment of the rotational speed of the air evaporator fan, of the scroll compressor, the openings of the expansion valves as well as the four-ways valves. The drive cooler is an additional heat exchanger installed to cool down the power electronic used for the variation of the compressor speed.

Conditions in terms of temperature and absolute pressure are measured at the supply/exhaust of each component of the refrigerant loop. Temperatures are determined by means of sensor pocket (type T thermocouple) with accuracy of ± 0.3 K. Used absolute pressure sensors show the following characteristics:

- Operating range of 0-20 bar for the sensor used at the supply of the compressor with an accuracy of 1% of the full scale range
- Operating range of 0-30 bar for sensors used for measuring the low and intermediate pressure level with an accuracy of $\pm 1\%$ of the full scale range,
- Operating range of 0-50 bar for sensors used for measuring the high pressure with an accuracy of $\pm 0.5\%$ of the full scale range.

The refrigerant flow rate at the exhaust of the liquid receiver is measured by means of a Coriolis flow meter with a relative error 0.1%. A heat exchanger (subcooler, SC) has been added in order to insure a small degree of subcooling under any working conditions and thus insure a better flow rate measurement. This subcooler is a 10 cm long concentric tube heat exchanger where the refrigerant in the inner tube can be cooled down with tap water.

The relative error related to the use of flow meter used for the determination of the refrigerant flow rate passing through the high pressure side economizer is also equal to 0.1%.

3.2. Water loop

Water flow rate passing through the condenser is controlled by adjusting the rotational speed of the water pump. The water temperature at the supply of the condenser is adjusted by a PID controlling the opening of a three-ways valve. This latter is supposed to mix a flow rate coming from the exhaust

of the condenser and another one coming from the water tank. This latter is used as a heat sink that can be either cooled continuously by means of tap water or heated up via variable electrical resistances. Given the low temperature difference between the supply and the exhaust of the condenser (between 3 and 10K), PT100 with accuracy of ± 0.1 K have been preferred instead of type T thermocouple. Water flow rate is determined by means of an impulse water meter (4 pulses per liter).

Table 2. List of sensors and related accuracy

Sensors	Error
Type T thermocouples	± 0.3 K
PT100 class 1/10 DIN	± 0.1 K
Keller 0-20 bar absolute pressure	± 0.2 bar
Keller 0-30 bar absolute pressure	± 0.3 bar
Keller 0-50 bar absolute pressure	± 0.25 bar
Krohne Optimass 6000	± 0.1 %
Emerson micro-motion CMF025	± 0.1 %
Impulse water meter	4 pulses per liter

3.3. Outdoor climate

The outdoor unit is installed in a room where conditions are controlled in terms of both humidity and temperature. Relative humidity is controlled by the use of electrical steam generators (humidifier). It is also possible to control with precision the outdoor air temperature by means of a set of variable electrical resistances. Outdoor unit conditions are controlled by means of a PID integrated in the Labview controller. An air mixing fan is used to ensure conditions homogeneity all over the outdoor room. The relative humidity at the inlet and at the outlet of the outdoor air stream passing through the air evaporator are measured by means of relative humidity sensors with an accuracy of ± 1.5 percent points.

4. Results

A steady state validation of the main components is presented in this section as well as a comparison between the system model predictions and the experimental results.

Observations on the superheat control are also presented and commented.

The heat pump was tested in a wide variety of working conditions presented in Tab. 3. The condensing and evaporating temperature are defined for a quality of 1 and respectively the pressure at the condenser inlet and at the evaporator exhaust.

Table 3. Testing conditions ranges

Variables	Min. Value	Max Value
Compressor speed [rpm]	3000	7000
Water inlet temperature [$^{\circ}$ C]	30.6	56.2
Water temperature increase [K]	4.3	9.5
Outside air temperature [$^{\circ}$ C]	-3	35
Condensing temperature [$^{\circ}$ C]	38	62
Heating capacity [W]	6200	12100
Evaporating temperature [$^{\circ}$ C]	-15.4	16.8

4.1. Steady-state validation

In order to validate the model, each component model had to be validated separately. This validation is detailed in the following subsections. The different mean absolute errors of the predictions of the component models are all given in Tab. 4 using the mean absolute percentage error (MAPE) and the mean absolute error (MAE).

Table 4. Errors on components models predictions

Variables	MAPE / MAE
Compressor electrical power	6.8%
Compressor discharge temperature	2.7 K
Suction mass flow rate	1.8%
Injection mass flow rate	17.8%
Heating capacity	2.6%
Cooling capacity	2.5%
Evaporator refrigerant outlet temperature	2.6 K
Economizer load	2.0%
Economizer intermediate pressure side outlet temperature	2.3 K
Heating valve mass flow rate	4.4%
Injection valve mass flow rate	5.7%

4.1.1. Condenser

In order to validate the condenser model, both secondary and working fluid mass flow rates were imposed to the experimental measurements. The condensing pressure and both inlet temperatures were also imposed, the main output of the model being the heating capacity (c.f. Fig. 3).

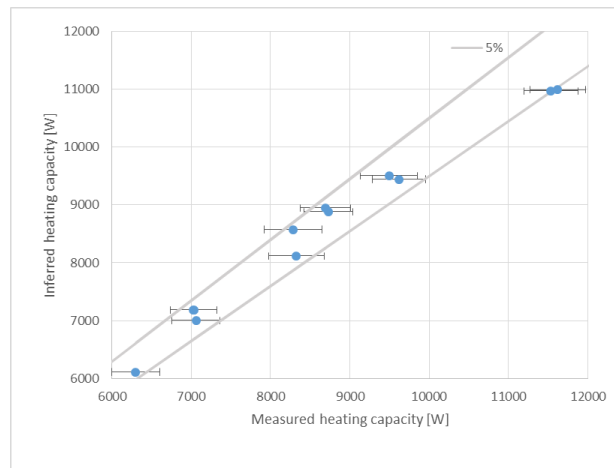


Fig. 3. Condenser heating capacity parity plot

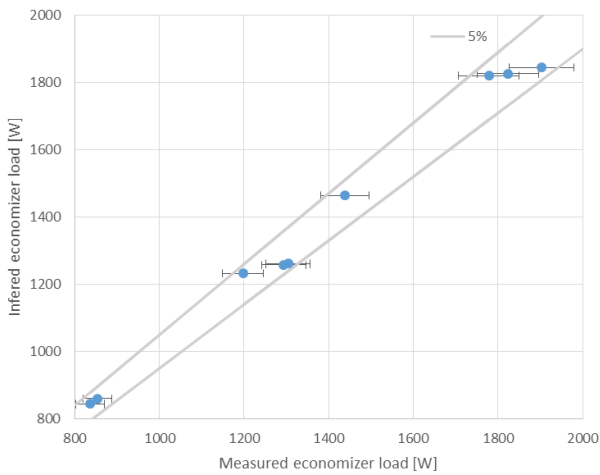
4.1.2. Economizer

Similarly to the condenser, the validation of the economizer model needs the mass flow rate, pressure and inlet enthalpy to be fixed on both the intermediate (IP) and high (HP) pressure side. The main outputs are then the economizer load [W] and the injection temperature, i.e. the intermediate pressure side outlet temperature (c.f. Fig. 4a and 4b).

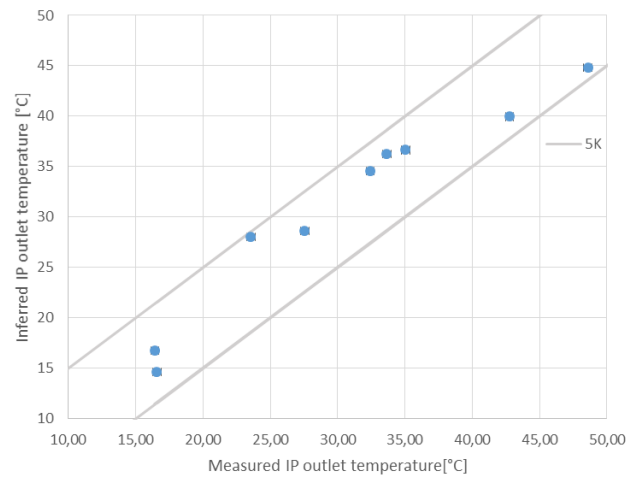
4.1.3. Evaporator

In this case, the mass flow rate, pressure and inlet enthalpy on both sides (air and working fluid) has to be fixed. Moreover, the inlet humidity ratio on the air side had also to be given. The parity plots of

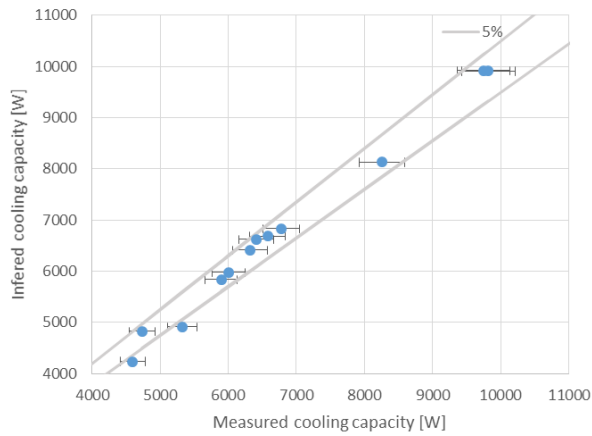
the model main outputs, i.e. the cooling capacity and the outlet temperature on the refrigerant side, are given in Fig. 4c and 4d.



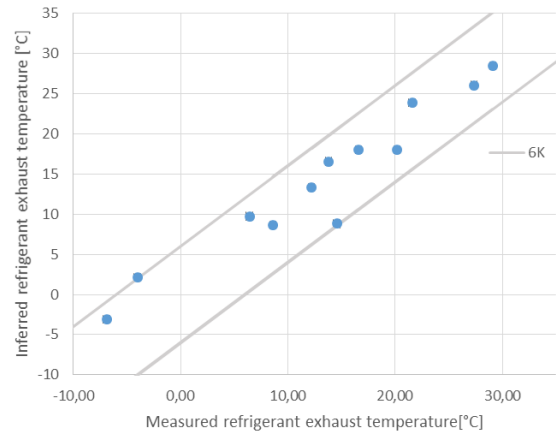
(a)



(b)



(c)

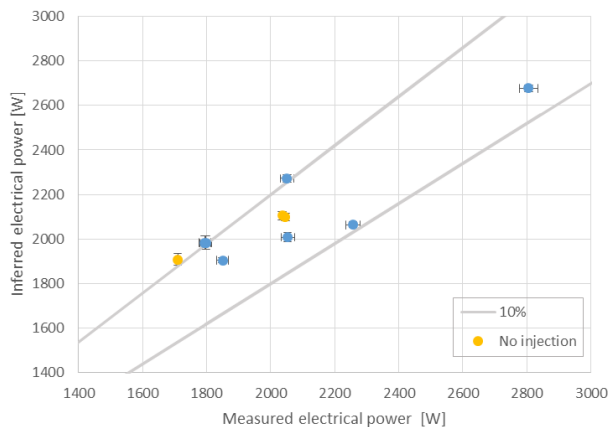


(d)

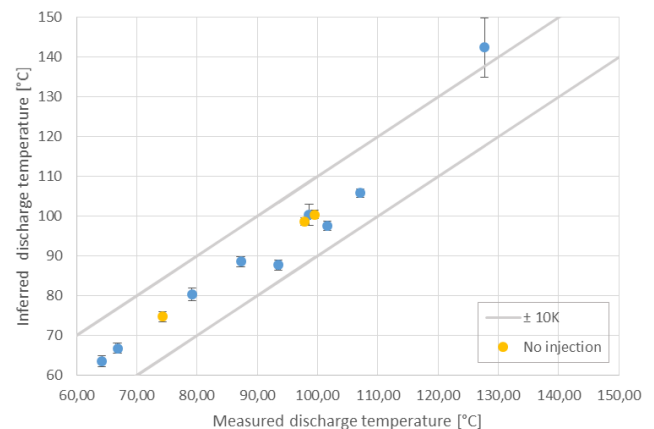
Fig. 4. Parity plots for: (a) Economizer load; (b) Economizer intermediate pressure side outlet temperature; (c) Cooling capacity; (d) Evaporator refrigerant outlet temperature

4.1.4. Compressor

In order to compare the compressor model with the experimental data, it was decided to impose the three pressure levels as well as the rotational speed. The outputs, i.e. the mass flow rates and the electrical power are compared against experimental data in Fig. 5. Points in yellow were conducted with the injection valve closed and thus no injection mass flow rate was measured. It can be seen that the prediction of the electrical power and the injection ratio is not ideal. A more physical model of the compressor could be developed.



(a)



(b)

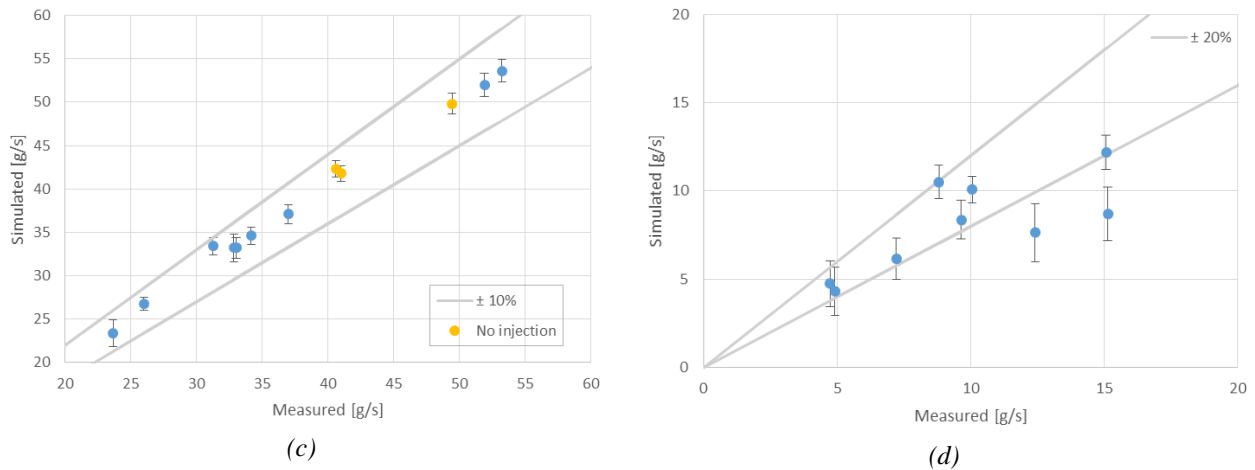


Fig. 5. Parity plots for: (a) electrical power; (b) discharge temperature; (c) suction mass flow rate; (d) injection mass flow rate

4.1.5. Expansion valves

The validation of the expansion valves model needs the pressure at the inlet and outlet of the valve to be fixed, as well as the opening. Moreover, the enthalpy at the inlet has also to be given. The model outputs the mass flow rate passing through the valve. The parity plots for both the injection and outdoor expansion valves are presented in Fig. 6.

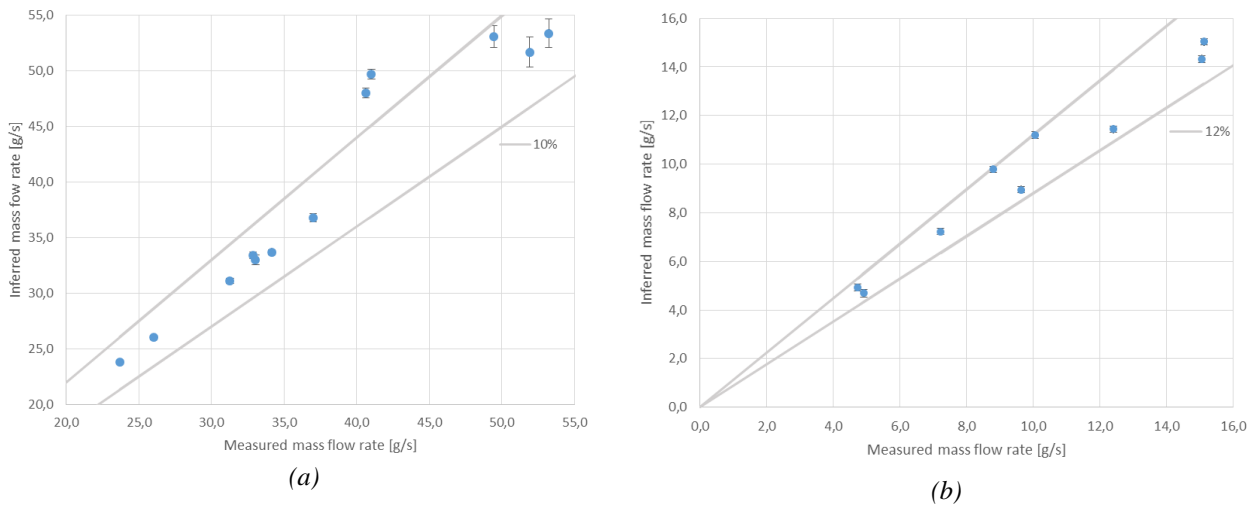


Fig. 6. Parity plots for: (a) outdoor mass flow rate; (b) injection mass flow rate

4.1.6. System

The inputs of the heat pump model (c.f. Fig. 1) are the secondary fluids (air and water) inlet mass flow rates, pressures and temperatures. The humidity ratio has also to be specified for the air. The compressor rotational speed and the EEVs openings are also inputs of the model. The mean absolute percentage error (MAPE) and the mean absolute error (MAE) are given in Tab. 5 for some key variables. It was observed that all heat transfer rate are overestimate due to a too large mass flow rate. This is mainly due to a higher inferred density at the suction port of the compressor.

Table 5. Errors on key outputs of the heat pump model

Variables	MAPE / MAE
Compressor electrical power	7%
Compressor discharge temperature	12.7 K
Heating capacity	14%

Cooling capacity
COP

17%
13%

3.2. Superheat control

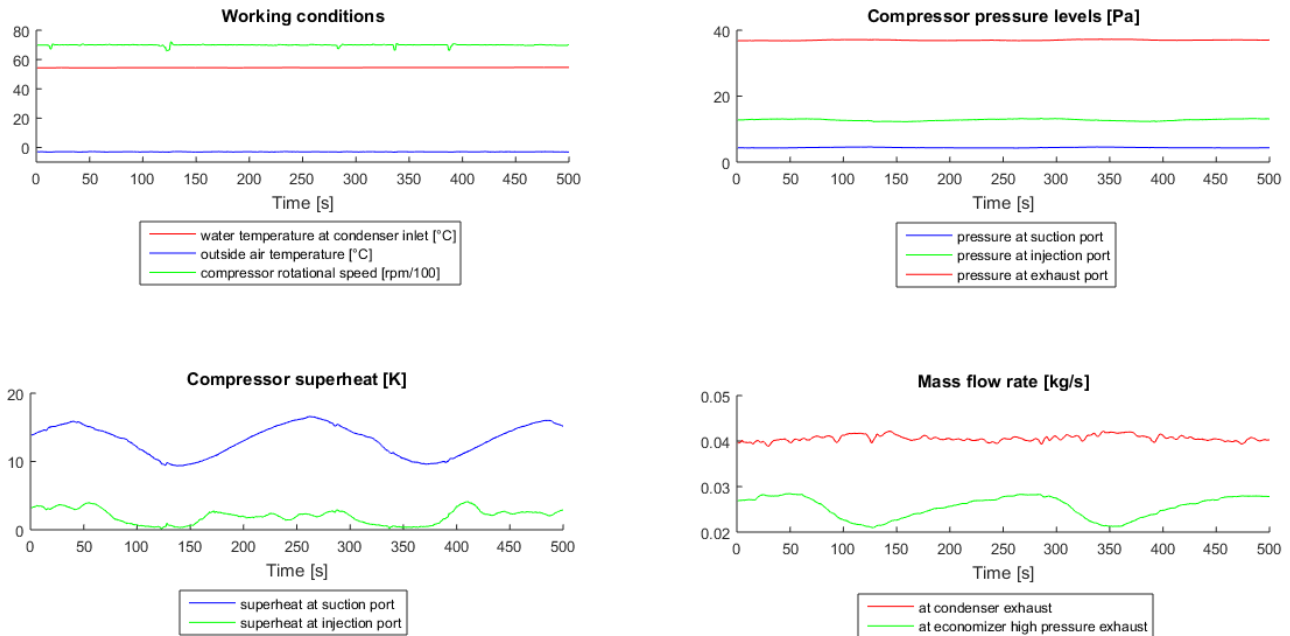


Fig. 4. Superheat control for steady operating conditions

Figure 3 shows experimental results where the control of the superheat can be observed. The first graph shows that the working conditions of the system are fixed as the rotational speed, the water inlet temperature and the outside air temperature are almost constant. However, it can be seen that the control of both superheats, on the suction and injection lines, is not optimum as the superheats are not stabilized. This is due to the fact that the current control uses a decoupled adaptive PID controller with no feed-forward action. The control of the superheat, especially on the suction line is made difficult by the presence of the suction line which has a significant impact on the response of the superheat at the suction of the compressor for a given variation of the valve opening.

It can be concluded that, because of the complexity of the system, the current controller could be improved and the developed dynamic model of the heat pump could help to design more advanced control strategies.

5. Conclusions & future work

Experimental results and a dynamic model of an air-source heat pump were presented. The control of the superheat, both for the injection and suction line could be improved. This is due to the complex dynamics associated with the vapor split line, the evaporator and the economizer. Furthermore, these systems are coupled and interact with each other.

This last observation yield to the conclusion that a dynamic model was needed in order to develop more advanced control. The steady state validation of the main component models was conducted. It was shown that the compressor model predictions for both the electrical consumed power and the injection mass flow rate could be improved.

Regarding the system model, improvements could be achieved by adding pressure drops, especially on the suction line in order to decrease the density at the suction and thus the mass flow rate.

It was also observed that using constant heat transfer coefficient values per zone did not affect greatly the prediction of the heat transfer rate of all the heat exchangers of the system.

The dynamic response of the presented model has to be validated against experimental data so that it could be used to develop model based or model predictive control.

Acknowledgments

The authors would like to acknowledge Emerson Climate Technologies who sponsored a part of the test bench.

References

- [1] Rasmussen, Bryan P. "Dynamic modeling for vapor compression systems - Part I: Literature review." *HVAC&R Research* 18, no. 5 (2012): 934-955.
- [2] Rasmussen, Bryan P., and Bhaskar Shenoy. "Dynamic modeling for vapor compression systems - Part II: Simulation tutorial." *HVAC&R Research* 18.5 (2012): 956-973.
- [3] Qiao, Hongtao, Xing Xu, Vikrant Aute, and Reinhard Radermacher. "Transient modeling of a flash tank vapor injection heat pump system - Part I: model development." *International Journal of Refrigeration* 49 (2015): 183-194.
- [4] Qiao, Hongtao, Xing Xu, Vikrant Aute, and Reinhard Radermacher. "Transient modeling of a flash tank vapor injection heat pump system Part II: Simulation results and experimental validation." *International Journal of Refrigeration* 49 (2015): 183-194.
- [5] Ling, Jiazhen; Qiao, Hongtao; Alabdulkarem, Abdullah; Aute, Vikrant; and Radermacher, Reinhard, "Modelica-based Heat Pump Model for Transient and Steady-State Simulation Using Low-GWP Refrigerants" (2014). International Refrigeration and Air Conditioning Conference. Paper 1421. <http://docs.lib.purdue.edu/iracc/1421>
- [6] Li, Bin, Ste_en Peuker, Predrag S. Hrnjak, and Andrew G. Alleyne. "Refrigerant mass migration modeling and simulation for air conditioning systems." *Applied Thermal Engineering* 31, no. 10 (2011): 1770-1779.
- [7] Quoilin, Sylvain; Desideri, Adriano; Wronski, Jorrit; Bell, Ian; and Lemort, Vincent, "ThermoCycle: Modelica library for the simulation of thermodynamic systems" (2014). *Proceedings - 10th International Modelica Conference*; doi:10.3384/ECP14096683
- [8] Bell, Ian H., Jorrit Wronski, Sylvain Quoilin, and Vincent Lemort. "Pure and pseudo-pure fluid thermophysical property evaluation and the open-source thermophysical property library Coolprop." *Industrial & engineering chemistry research* 53, no. 6 (2014): 2498-2508.
- [9] Kwan-Soo Lee, Woo-Seung Kim, and Tae-Hee Lee. A one-dimensional model for frost formation on a cold at surface. *International Journal of Heat and Mass Transfer*, 40(18):4359-4365, 1997.
- [10] Dechesne, Bertrand; Bertagnolio Stéphane; and Vincent Lemort. "Empirical model of a variable speed vapor injection compressor for air source heat pump dynamic modeling." *International conference on compressors and their systems*. 2015.
- [11] Bach, Christian K.; Braun, James E.; and Groll, Eckhard A., "A Virtual EXV Mass Flow Sensor for Applications With Two-Phase Flow Inlet Conditions" (2012). *International Refrigeration and Air Conditioning Conference*. Paper 2122.
- [12] Park, Chasik, Honghyun Cho, Yongtaek Lee, and Yongchan Kim. "Mass flow characteristics and empirical modeling of R22 and R410A owing through electronic expansion valves." *International Journal of Refrigeration* 30, no. 8 (2007): 1401-1407.
- [13] Christian JL Hermes, Robson O Piucco, Jader R Barbosa, and Claudio Melo. A study of frost growth and densication on at surfaces. *Experimental Thermal and Fluid Science*, 33(2):371-379, 2009.
- [14] Xu, Xing, Yunho Hwang, and Reinhard Radermacher. "Refrigerant injection for heat pumping/air conditioning systems: literature review and challenges discussions." *International Journal of Refrigeration* 34.2 (2011): 402-415.